

Published in final edited form as:

*Arterioscler Thromb Vasc Biol.* 2012 May ; 32(5): 1178–1185. doi:10.1161/ATVBAHA.111.244186.

## ICAM-1 engagement modulates sphingomyelinase and ceramide, supporting uptake of drug carriers by the vascular endothelium

Daniel Serrano<sup>1</sup>, Tridib Bhowmick<sup>2</sup>, Rishi Chadha<sup>2</sup>, Carmen Garnacho<sup>2</sup>, and Silvia Muro<sup>2,3</sup>

<sup>1</sup>Department of Cell Biology & Molecular Genetics and Biological Sciences Graduate Program, University of Maryland, College Park, MD

<sup>2</sup>Institute for Biosciences & Biotechnology Research, University of Maryland, College Park, MD

<sup>3</sup>Fischell Department of Bioengineering, University of Maryland, College Park, MD

### Abstract

**Objective**—Engagement of intercellular adhesion molecule 1 (ICAM-1) on endothelial cells (ECs) by ICAM-1-targeted carriers induces cell adhesion molecule (CAM)-mediated endocytosis, providing intra-endothelial delivery of therapeutics. This pathway differs from classical endocytic mechanisms and invokes aspects of endothelial signaling during inflammation. ICAM-1 interacts with Na<sup>+</sup>/H<sup>+</sup> exchanger NHE1 during endocytosis, but it is unclear how this regulates plasmalemma and cytoskeletal changes. We studied such aspects in this work.

**Methods and Results**—We used fluorescence and electron microscopy, inhibitors and knockout tools, cell culture and mouse models. ICAM-1 engagement by anti-ICAM carriers induced sphingomyelin-enriched engulfment structures. Acid sphingomyelinase (ASM), an acidic enzyme that hydrolyzes sphingomyelin into ceramide (involved in plasmalemma deformability and cytoskeletal reorganization), redistributed to ICAM-1-engagement sites at ceramide-enriched areas. This induced actin stress fibers and carrier endocytosis. Inhibiting ASM impaired ceramide enrichment, engulfment structures, cytoskeletal reorganization, and carrier uptake, which was rescued by supplying this enzyme activity exogenously. Interfering with NHE1 rendered similar outcomes, suggesting that Na<sup>+</sup>/H<sup>+</sup> exchange might provide an acidic microenvironment for ASM at the plasmalemma.

**Conclusions**—These findings are consistent with the ability of ECs to internalize relatively large ICAM-1-targeted drug carriers, and expand our knowledge on the regulation of the sphingomyelin/ceramide pathway by the vascular endothelium.

### Keywords

ICAM-1; CAM-mediated endocytosis; acid sphingomyelinase; ceramide/sphingomyelin pathway; actin cytoskeleton

---

Corresponding author: Silvia Muro, 5115 Plant Sciences Building, University of Maryland, College Park, MD 20742, muro@umd.edu, Phone/Fax: 301-405-4777 / 301-314-9075.

**Publisher's Disclaimer:** This is a PDF file of an unedited manuscript that has been accepted for publication. As a service to our customers we are providing this early version of the manuscript. The manuscript will undergo copyediting, typesetting, and review of the resulting proof before it is published in its final citable form. Please note that during the production process errors may be discovered which could affect the content, and all legal disclaimers that apply to the journal pertain.

The authors declare no disclosures.

Intercellular adhesion molecule 1 (ICAM-1) is an immunoglobulin-like transmembrane glycoprotein predominantly present on endothelial cells (ECs)<sup>1, 2</sup>. It is over-expressed in vascular pathologies involving inflammation, thrombosis, atherosclerosis, oxidative stress, ischemia-reperfusion, altered blood flow, and diabetes<sup>1, 2</sup>, representing an interesting target for vascular drug delivery<sup>3-5</sup>. Multivalent engagement of ICAM-1 by anti-ICAM-coated polymer carriers used for targeting of therapeutics, results in uptake of said carriers via cell adhesion molecule (CAM)-mediated endocytosis (supplemental Table S1)<sup>6</sup>. This provides intra-endothelial delivery of therapeutics in cell culture and animal models<sup>7-11</sup>. Knowledge of the regulatory pathways underlying this process is hence valuable for the design of more effective intravascular treatments.

CAM-mediated endocytosis depends on dynamin, a GTPase involved in budding of clathrin- and caveolar-associated vesicles, yet materials internalized via ICAM-1 do not co-localize with these markers and their uptake is not affected by inhibiting these routes<sup>6, 12, 13</sup>. CAM-mediated endocytosis requires protein kinase C (PKC), but not phosphatidylinositol 3 kinase (PI3 kinase) or phospholipase C (PLC) that are involved in macropinocytosis and phagocytosis<sup>6</sup>. It also involves Src kinases and Rho-dependent kinase (ROCK), leading to actin stress fibers formation<sup>6</sup>, but not actin cups or microtubules observed in macropinocytosis and phagocytosis<sup>14, 15</sup>. This pathway is also associated to platelet-endothelial cell adhesion molecule 1 (PECAM-1)<sup>6</sup>, but differs from clathrin-mediated uptake of E-selectin<sup>16</sup>, P-selectin<sup>17</sup>, or vascular cell adhesion molecule 1 (VCAM-1)<sup>18</sup>, and caveolar-mediated turnover of thrombomodulin<sup>19</sup>. ICAM-1 pathway may be related to other non-classical endocytic routes, such as that of fibroblast growth factors mediated by syndecans<sup>20</sup>, yet this remains unexplored.

Upon multivalent engagement by anti-ICAM carriers, ICAM-1 interacts with amiloride-sensitive Na<sup>+</sup>/H<sup>+</sup> exchanger protein NHE1<sup>21</sup>. NHE1 can serve as a cytoskeleton adaptor through ezrin/radixin/moesin (ERM) proteins and  $\alpha$ -actinin<sup>22</sup>, leading to alignment of actin bundles beneath carrier particles<sup>21</sup>. This contributes to formation of membrane engulfing structures and invaginations, leading to internalization of objects ranging from ~180 nm to ~5  $\mu$ m in diameter, providing a remarkable flexibility for design of drug carriers<sup>9</sup>.

It is likely that uptake of said drug carriers by ECs requires not only specialized cytoskeletal structures but also lipid platforms providing reduced diffusion of the involved elements (ICAM-1, NHE1, the cytoskeleton, and signaling molecules). This has been observed during engagement of ICAM-1 by leukocyte  $\beta_2$  integrins, which also involves PKC and Src kinase, actin stress fibers, and specialized lipid domains on the EC surface<sup>23, 24</sup>.

Yet, CAM-mediated endocytosis remains relatively uncharacterized. In this work, we studied the regulatory link between plasmalemma and cytoskeletal elements involved in endocytosis via ICAM-1. We found an unforeseen role for acid sphingomyelinase (ASM) and the sphingomyelin/ceramide pathway in this process, with NHE1 providing a ground for spatial regulation of these events. Our data are consistent with the ability of ECs to internalize relatively large drug carriers bound to ICAM-1, and also expand the knowledge of the role of the sphingomyelin/ceramide pathway on the function of the vascular endothelium.

## Methods

### Antibodies and reagents

Antibodies to human or mouse ICAM-1 were R6.5 and phycoerythrin-LB-2 (Santa Cruz Biotechnology, Santa Cruz, CA), or YN1, respectively<sup>7</sup>. Antibodies to PECAM-1, NHE1, VCAM-1, clathrin heavy chain, mannose 6-phosphate receptor (M6PR), ASM, ganglioside

GM1, or ceramide were from BD Biosciences (Franklin Lakes, NJ), EMD Chemicals (Gibbstown, NJ), Millipore (Billerica, MA), or Sigma-Aldrich (Saint Louis, MO). Secondary antibodies were from Jackson ImmunoResearch (West Grove, PA). Polystyrene-latex beads were from Polysciences (Warrington, PA). BODIPY® FL C12-sphingomyelin and Texas Red-labeled phalloidin were from Molecular Probes (Eugene, OR). Human recombinant ASM was provided by Dr. Edward Schuchman (Mount Sinai School of Medicine, New York, NY) and neutral SM was from Sigma-Aldrich. All other reagents were from Sigma-Aldrich.

### Cell cultures

Human umbilical vein endothelial cells (HUVECs) from Lonza (Walkersville, MD) were cultured in supplemented M-199 medium<sup>6</sup>. Mouse lung ECs (MLECs) were isolated from wild-type C57BL/6 (The Jackson Laboratory, Bar Harbor, ME) or ASM<sup>-/-</sup> mice<sup>25</sup> (provided by Dr. Schuchman) using magnetic beads coated with anti-PECAM-1, and cultured in supplemented DMEM<sup>26</sup>. Cells were seeded on 1%-gelatin-coated coverslips and treated overnight with 10 ng/mL TNF $\alpha$  to induce ICAM-1 over-expression<sup>6</sup>.

### Preparation of polymer carriers targeted to cell surface markers

Model carriers were prepared by adsorbing antibodies to ICAM-1, VCAM-1, or M6PR on the surface of 4.5  $\mu\text{m}$  (or 100 nm, when indicated) diameter polystyrene, as described<sup>6, 9, 27, 28</sup>, rendering ~5,000 (or ~7,000) antibody molecules/ $\mu\text{m}^2$ , equivalent to ~320,000 (or ~250) antibody molecules/particle. Alternatively (when indicated), 4.5  $\mu\text{m}$  carriers were prepared using a 50:50 mass-ratio mix of anti-ICAM and IgG or recombinant ASM (~2,500 anti-ICAM molecules/ $\mu\text{m}^2$ ).

### Enrichment of lipids at sites of ICAM-1 engagement on the endothelial plasmalemma

Anti-ICAM carriers were incubated for 15 min at 37°C with control HUVECs or HUVECs treated with 5 mM methyl- $\beta$ -cyclodextrin (Cdx, to extract cholesterol), 20  $\mu\text{M}$  5-(N-ethyl-N-isopropyl)amiloride (EIPA, to inhibit NHE1), 50  $\mu\text{M}$  imipramine (to inhibit ASM), or a mix of 50  $\mu\text{M}$  imipramine and 500 mU/mL neutral SM (to inhibit ASM while providing SM activity). Non-bound carriers were washed and cells were fixed. Carrier engulfment by ECs was verified by scanning electron microscopy (SEM). In parallel, cholesterol was stained using 50  $\mu\text{g/mL}$  filipin, and sphingomyelin was visualized by pre-incubating HUVECs with 0.2  $\mu\text{g/mL}$  BODIPY®-sphingomyelin<sup>9</sup>. Ganglioside GM1 and ceramide were immunostained. Cell-bound carriers were identified by phase-contrast microscopy, and enrichment of molecules at these sites was quantified as the fold-increase of fluorescence intensity at engulfment structures (~2  $\mu\text{m}$  above the cell surface) over that of adjacent regions, as described in the Data Supplement.

### Recruitment of proteins at sites of ICAM-1 engagement on the endothelial plasmalemma

Anti-ICAM, anti-VCAM, or anti-M6PR carriers were incubated for 15 or 30 min at 37°C with control HUVECs or HUVECs treated with 5 mM Cdx (to remove cholesterol), 50  $\mu\text{M}$  imipramine (to inhibit ASM), a mix of 50  $\mu\text{M}$  imipramine and 500 mU/mL neutral SM (to inhibit ASM while providing SM activity), 3 mM amiloride or 20  $\mu\text{M}$  EIPA (to inhibit NHE1), 0.5  $\mu\text{M}$  wortmannin (to inhibit PI3 kinase), or 10  $\mu\text{M}$  1-(5-isoquinolinylsulfonyl)-2-methyl-piperzine (H-7, to inhibit PKC). Anti-ICAM-coat on carriers was detected by immunofluorescence. ASM, ICAM-1, NHE1, M6PR and VCAM-1 were also immunostained for fluorescence microscopy. Semi-quantitative analysis of the enrichment of these molecules at sites of carrier binding was performed as described above.

The intracellular distribution of ASM was assessed by computing the total number of ASM-positive vesicles (~100–300 nm diameter) and those located within 5  $\mu\text{m}$  distance around the nucleus (perinuclear). Peripheral intracellular ASM was calculated as the number of total – perinuclear ASM-positive vesicles.

Co-precipitation of ASM,  $\alpha$ -actinin, and moesin with ICAM-1 was assessed by incubating HUVECs with anti-ICAM magnetic beads for 15 min at 37°C as described<sup>21</sup>, followed recovery of bound beads, protein elution and separation by electrophoresis, and liquid chromatography/mass spectrometry.

### Actin remodeling and CAM-mediated endocytosis

Formation of filamentous actin (F-actin) upon binding of anti-ICAM carriers to HUVECs over a period of 15 min at 37°C, was visualized by fluorescence microscopy using Alexa Fluor 594-phalloidin.

For endocytosis in cell cultures, HUVECs, wild-type MLECs, or ASM<sup>-/-</sup> MLECs were incubated at 37°C with anti-ICAM carriers for 30 min to allow binding, followed by washing of non-bound carriers and incubation at 37°C for 1 h to allow endocytosis. Similar tests were performed in 3 mM amiloride, 50  $\mu\text{M}$  imipramine, 0.5  $\mu\text{M}$  wortmannin, 10  $\mu\text{M}$  H-7, or Na<sup>+</sup>-depleted solution (138 mM choline chloride, 5.4 mM KCl, 1 mM CaCl<sub>2</sub>, 1 mM MgCl<sub>2</sub>). Endocytosis of carriers displaying 50% anti-ICAM surface-density was also tested, as well as the effect of co-coating carriers with both anti-ICAM and recombinant ASM, to rescue this activity. After cell fixation, carriers accessible at the cell surface were counter-stained using Texas Red-labeled secondary antibody, and the number of carriers internalized per cell was quantified by phase-contrast (total carriers) and fluorescence microscopy (surface-located carriers), as described<sup>6, 9</sup>.

C57BL/6, caveolin-1<sup>-/-</sup> or ASM<sup>-/-</sup> mice were anesthetized intraperitoneally with 100/10 mg/kg body-weight ketamine/xylazine and injected intravenously with ~180 nm anti-ICAM carriers (instead of 4.5  $\mu\text{m}$  counterparts that may cause embolization). Intracardial perfusion 3 h after injection was used to remove circulating carriers and carriers loosely bound the vasculature, and lungs were processed into 80–90 nm-thin resin-embedded sections to visualize the pulmonary endothelium by transmission electron microscopy (TEM)<sup>9</sup>. Endocytosis of anti-ICAM carriers by pulmonary ECs *in vivo* was semi-quantitatively assessed as the number of EC internalized carriers per field, as described<sup>29</sup>. All animal studies adjusted to IACUC regulations.

### Statistics

Data are means  $\pm$  standard error of the mean (s.e.m.). Statistical significance was determined by Student's *t*-test.

(Additional descriptions on Methods are provided in the Data Supplement).

## Results

### Visualization of lipid components at sites of engulfment of anti-ICAM carriers by endothelial cells

To visualize the cell surface and enrichment of particular molecules during the initial steps of CAM-mediated endocytosis, we looked at the interaction of 4.5  $\mu\text{m}$  anti-ICAM carriers with the EC plasmalemma. Fluorescence microscopy showed that, within 15 min, anti-ICAM carriers bound to ECs and were engulfed (confirmed by SEM; Figure 1A) by ICAM-1-enriched membrane protrusions (Video 1 and Figure 1B).

Next, we visualized lipid-raft components, since ICAM-1 crosslinking with antibodies elicits its association with detergent-resistant membrane fractions<sup>30</sup>. Cholesterol, sphingomyelin, and ganglioside GM1 were enriched by  $1.5\pm 0.05$ -fold,  $2.5\pm 0.1$ -fold, and  $3.2\pm 0.1$ -fold, respectively, in regions of carrier engulfment versus adjacent “background” areas (Figure 1C and supplemental Figure S1A). Cholesterol removal by methyl- $\beta$ -cyclodextrin (Cdx; top panels of Figure 1D and supplemental Figure 1B) impaired engulfment, reflected by reduced ICAM-1 signal around carriers (39.8% reduction; middle and bottom panels in Figure 1D and supplemental Figure 1B), and confirmed by SEM (Supplemental Figure S2). NHE1 inhibition by amiloride (supplemental Figure S3) also resulted in a 29.2% reduction in carrier engulfment. Neither Cdx nor amiloride affected binding of anti-ICAM carriers to ECs (compare phase-contrast in Figure 1C–D top panels or those in supplemental Figure S3). These results suggest the need for an appropriate lipid environment and NHE1 function for successful endothelial engulfment of anti-ICAM carriers.

### Effect of impairing acid sphingomyelinase on CAM-mediated endocytosis

The role of cholesterol/sphingomyelin-rich domains and NHE1 (a linker between CAM-mediated endocytosis and the cytoskeleton<sup>21, 22</sup>) in the first stages of anti-ICAM carrier uptake suggests involvement of ASM. This enzyme hydrolyzes sphingomyelin into ceramide<sup>31, 32</sup>, which supports large lipid domains<sup>33, 34</sup>, favors vesiculation<sup>34–36</sup>, and promotes cytoskeletal rearrangement<sup>37, 38</sup> associated to several physiological functions<sup>39</sup>. ASM inhibition by imipramine decreased endothelial endocytosis of anti-ICAM carriers (~38% reduction; Figure 2A). Endocytosis was also affected by inhibiting NHE1 with amiloride (~86% reduction), but not by inhibiting caveolar-mediated endocytosis with filipin (~7% increase) or by reducing anti-ICAM surface-density on carriers by 50%, which only affected binding (59% reduction; data not shown). Confirming a role for ASM, endothelial endocytosis of anti-ICAM carriers was also impaired in ECs isolated from ASM<sup>-/-</sup> mice (75% reduction versus wild-type; Figure 2A), yet uptake was rescued by co-coating recombinant ASM onto anti-ICAM carriers (147% uptake compared to wild-type; Figure 2A).

This finding was validated *in vivo* after intravenous injection of anti-ICAM carriers (~180-nm, to avoid potential embolization by 4.5- $\mu$ m carriers) in wild-type, caveolin-1<sup>-/-</sup>, or ASM<sup>-/-</sup> mice, followed by visualization and semi-quantitative estimation of carrier endocytosis by pulmonary ECs (a preferential target for anti-ICAM carriers) using TEM, as recently described<sup>29</sup>. In agreement with cell culture experiments, endocytosis of anti-ICAM carriers was inhibited in ASM<sup>-/-</sup> mice but not in caveolin-1<sup>-/-</sup> mice (12.2% and 92.8% of wild-type mice, respectively; Figure 2B). This verifies that ASM is required for endocytosis of anti-ICAM carriers by the vascular endothelium.

### Recruitment of acid sphingomyelinase, ceramide generation, and role of NHE1 at sites of engulfment of anti-ICAM carriers by endothelial cells

We then determined whether ASM is involved in CAM-mediated endocytosis through ceramide generation at sites of carrier engulfment by ECs. Immunofluorescence showed that, in the absence of anti-ICAM carriers, most ASM localized in the perinuclear region of cells, with a fraction located to vesicular-like structures ( $41.8\pm 4.7$  vesicles/cell; supplemental Figure S4) and few ASM-positive vesicles found outside this perinuclear area ( $23.7\pm 3.3$  vesicles/cell). ICAM-1 engagement by anti-ICAM carriers induced appearance of ASM-positive vesicles at the cell periphery (2.3-fold increase at 30 min), and carrier engulfment areas became enriched in ASM (Figure 3A). Confirming the specificity of this, ASM was not recruited to sites of carrier binding to VCAM-1, another cell adhesion molecule involved in inflammation, or mannose-6-phosphate receptor (M6PR), involved in



clathrin-mediated transport of ASM, (Figure 3A). Anti-M6PR carriers induced recruitment neither of ICAM-1 nor NHE1, but recruited clathrin heavy chain (supplemental Figure S5), validating this model.

ASM staining co-localized with ICAM-1 at areas of anti-ICAM carrier engulfment ( $85.1 \pm 2.9\%$  of carriers; Figure 3B), where ASM appeared within ICAM-1-lined vesicular structures (Figure 3B, 16X panel). However, opposite to  $\alpha$ -actinin or moesin, ASM did not co-immunoprecipitate with ICAM-1 (supplemental Table S2). This suggests that, upon release from intracellular vesicles, the enzyme simply interacts with sphingomyelin at neighboring sites of the plasmalemma rather than ICAM-1.

Importantly, ceramide also became enriched at these sites ( $3.5 \pm 0.01$ -fold over adjacent regions; Figure 4A and Supplemental Figure S6A), which was impaired by inhibiting ASM with imipramine (23.6% decrease), and rescued by exogenously added neutral SM (92% of control). Similarly, EIPA (an amiloride derivative that specifically inhibits NHE1<sup>21</sup>) also reduced ceramide enrichment (35.6% decrease), suggesting that this ion exchanger, which mediates H<sup>+</sup> efflux, may provide the acidic environment for ASM activity at the plasmalemma. Indeed, ASM staining also co-localized with NHE1 ( $85.3 \pm 3.4\%$  of carriers; Figure 4B), and both ASM inhibition with imipramine and NHE1 inhibition with EIPA affected similarly carrier engulfment (37.9% and 36.6% decrease, respectively; Figure 4C and supplemental Figure S6B), which was rescued by exogenous neutral SM (87.8% of control). Further, Na<sup>+</sup> depletion (to impair Na<sup>+</sup>/H<sup>+</sup> transport) led to a 93% reduction in CAM-mediated endocytosis (Figure 2A). This suggests that NHE1 may connect the ASM-mediated sphingomyelin/ceramide pathway to CAM-mediated endocytosis.

### Effect of impairing acid sphingomyelinase on CAM-mediated actin rearrangement

As described for other systems<sup>33–36</sup>, ASM-mediated production of ceramide upon ICAM-1 engagement may contribute to formation of lipid domains (Figures 1 and 4) and vesiculation, resulting in endocytosis (Figure 2). This pathway is also known to promote cytoskeletal rearrangement<sup>38</sup>, a requirement for CAM-mediated uptake<sup>6, 9, 21</sup>.

In accord with this, ASM inhibition by imipramine hindered formation of actin stress fibers induced by anti-ICAM carriers (Figure 5A), as previously observed in the case of NHE1 inhibition by amiloride or EIPA<sup>21</sup>. Imipramine did not affect ASM recruitment to carrier-binding sites ( $93.4 \pm 5\%$  of control), yet it inhibited uptake of anti-ICAM carriers (Figure 2A), suggesting that ASM recruitment preceded ICAM-1-dependent cytoskeletal rearrangement. Confirming this, inhibition of PKC, which regulates actin stress fiber formation by CAM-mediated endocytosis, did not affect ASM recruitment to ICAM-1 binding sites, but inhibited carrier uptake (Figure 5B). In contrast, these events were independent of PI3 kinase (Figure 5B), previously shown to play no role in CAM-mediated uptake<sup>6</sup>.

## Discussion

Binding of anti-ICAM carriers to endothelial ICAM-1 leads to intracellular transport of said carriers via CAM-mediated endocytosis (Supplemental Table S1)<sup>6, 9</sup>. This pathway supports delivery of therapeutics into the vascular endothelium by means of carrier particles ranging from ~180-nm to several micrometers in diameter<sup>6, 9</sup>, and shows regulatory elements (signaling molecules, cytoskeletal reorganization<sup>6, 21</sup>) reminiscent of those elicited upon ICAM-1 engagement by leukocytes during inflammation<sup>40–42</sup>.

Here, we found that this process occurs at specialized lipid domains on the EC plasmalemma, where anti-ICAM carriers co-localized with ICAM-1-positive engulfment

structures. This occurred in areas enriched in cholesterol, sphingomyelin, and gangliosides, and was inhibited by disrupting said domains by cholesterol chelation. While this was expected, we found an unforeseen contribution by ASM and the sphingomyelin/ceramide pathway towards the formation of ICAM-1-enriched membrane protrusions and CAM-mediated endocytosis. ICAM-1 engagement led to ASM redistribution from perinuclear regions to plasmalemma sites where engulfment structures formed. ASM inhibition impaired ceramide enrichment at carrier-binding sites, actin re-organization, and carrier endocytosis, which was rescued by supplying this activity exogenously. Based on our data, we speculate that this enzyme is exocytosed from lysosomal compartments, yet this remains to be tested. It is known that lysosomes carrying ASM can be exocytosed<sup>36</sup>, providing a possible mechanism for our observation. Indeed, exocytosis of lysosomal ASM requires increased intracellular  $\text{Ca}^{2+}$ <sup>43</sup>, a phenomenon involved in CAM-mediated endocytosis<sup>21</sup>.

Ceramide also accumulated at areas of endothelial engulfment of anti-ICAM carriers, in accord with the presence of sphingomyelin and ASM, and inhibition of ceramide enrichment at these sites resulted in poor engulfment. Although the ceramide type associated to the ICAM-1 pathway remains to be elucidated, several ceramides impact the molecular and biophysical features of the plasmalemma, for instance, by promoting the formation of large lipid domains, affecting membrane function<sup>33, 34</sup>. Ceramide production by ASM at the outer leaflet of the plasma membrane also favors vesiculation<sup>34, 36</sup> and promotes cytoskeletal rearrangement<sup>38</sup>, suggesting that a similar pathway may contribute to formation of engulfment structures and vesicles supporting uptake of anti-ICAM carriers by ECs, as observed in this work.

Sphingomyelinase-mediated formation of ceramide domains at the plasmalemma is associated with phosphorylation and redistribution of actin-adapters of the ERM family, followed by conversion of ceramide into sphingosine-1-phosphate (S1P) and hyperphosphorylation of ERMs, finally culminating in the formation of membrane protrusions<sup>44</sup>. ICAM-1 redistributes to detergent-resistant membrane fractions upon crosslinking with antibodies and it co-precipitates with ERM proteins<sup>24</sup>, as also observed here. Thus, it is possible that CAM-mediated endocytosis proceeds through a similar mechanism.

NHE1 might provide a bridge among ICAM-1 engaged by anti-ICAM carriers, ASM activity and the sphingomyelin/ceramide pathway, and the re-organization of the actin cytoskeleton supporting carrier engulfment and endocytosis. NHE1 is involved in cytoskeletal rearrangement<sup>22</sup> and may crosslink actin filaments to the ICAM-1 cytosolic domain<sup>21</sup>. Its ion exchange activity also regulates elasticity at the endothelial surface<sup>45</sup>, explaining engulfment and endocytosis of micron-sized objects targeted to ICAM-1. Since ICAM-1 interacts with NHE1 upon binding of anti-ICAM carriers<sup>21</sup>, and due to the directionality of NHE1 ion exchange ( $\text{H}^+$  efflux)<sup>21, 46</sup>, NHE1 might create an acidic microenvironment at ICAM-1 engagement regions. Although there is controversy concerning the pH range at which exocytosed ASM can exert activity<sup>31, 36</sup>, NHE1 contribution would explain how this acidic enzyme can display activity at the otherwise neutral extracellular environment, and how ECs might regulate ceramide production with spatial precision. A similar function of NHE1 has been shown for other pH-sensitive enzymes<sup>46</sup>. Particularly, NHE1 inhibition with cariporide ameliorates cisplatin-induced, ASM-dependent generation of ceramide<sup>47</sup>.

Altogether, these data (complemented by data reported previously) suggest a model by which engagement of ICAM-1 in lipid domains enriched in sphingomyelin induces exocytosis of ASM to these areas of the endothelial plasmalemma (Figure 6). Engaged ICAM-1 forms a complex with NHE1, resulting in local acidification and ASM-driven

hydrolysis of sphingomyelin into ceramide. This favors actin polymerization and cytoskeleton remodeling, stabilizes the engagement platform by restricting molecular diffusion and providing cytoskeletal anchorage, regulates membrane deformability, and favors formation of engulfment structures and endocytic vesicles. These events support the ability of ECs to internalize relatively large drug carriers targeted to ICAM-1, as opposed to classical clathrin- or caveolar-mediated endocytosis. Results shown here and previously<sup>6, 9, 11, 27, 48</sup> also indicate that multivalent binding to ICAM-1 is required to induce these events, yet this is still achievable with carriers displaying different antibody surface-densities, emphasizing the design flexibility of this strategy.

These results hold relevance regarding inflammation and vascular pathologies. ECs constitutively secrete ASM, whose activity increases in inflammation and accelerates progression of atherosclerotic lesions<sup>49–51</sup>. Ceramide production by sphingomyelinases has also been associated to increased redox signaling and leukocyte attachment to brain endothelium<sup>52, 53</sup>. Leukocyte influx into alveoli is decreased upon ASM inhibition<sup>54</sup>, and metabolic imbalances causing high levels of ceramide can lead to higher leukocyte levels in tissue<sup>55</sup>. Leukocyte transmigration across the endothelium has been linked to cholesterol-, sphingomyelin-, and/or ganglioside-rich areas in lipid rafts<sup>30</sup>. Hence, our data showing redistribution of ASM to endothelial structures where ICAM-1 is engaged, along with enrichment of ceramide in these regions, are consistent with this literature.

These results advance current knowledge on the regulation of CAM-mediated endocytosis, which may provide new tools for modulation of intra-endothelial therapies, and also underscore the implication of sphingomyelin/ceramide signaling in the vascular function.

## Supplementary Material

Refer to Web version on PubMed Central for supplementary material.

## Acknowledgments

We thank Dr. Edward Schuchman (Mount Sinai School of Medicine, New York, NY) for providing ASM<sup>-/-</sup> mice and human recombinant ASM, as well as the Maryland NanoCenter, the Laboratory for Biological Ultrastructure, and the Proteomics Core Facility (University of Maryland, College Park, MD) for technical assistance.

This work was funded by a NSF Graduate Research Fellowship (D.S.), and grants AHA 09BGIA2450014 and NIH R01-HL098416 (S.M.).

## References

1. Rothlein R, Dustin ML, Marlin SD, Springer TA. A human intercellular adhesion molecule (ICAM-1) distinct from LFA-1. *J Immunol.* 1986; 137:1270–1274. [PubMed: 3525675]
2. Muro, S. Intercellular Adhesion Molecule-1 and Vascular Cell Adhesion Molecule-1. In: Aird, WC., editor. *Endothelial Biomedicine*. New York: Cambridge University Press; 2007.
3. Muro, S.; Muzykantov, V. Design Parameters Modulating Intracellular Drug Delivery: Anchoring to Specific Cellular Epitopes, Carrier Geometry, and Use of Auxiliary Pharmacological Agents. In: Weissig, V.; D'Souza, GG., editors. *Organelle-Specific Pharmaceutical Nanotechnology*. New Jersey: Wiley; 2010.
4. Sucusky P, Balachandran K, Elhammali A, Jo H, Yoganathan AP. Altered shear stress stimulates upregulation of endothelial VCAM-1 and ICAM-1 in a BMP-4- and TGF-beta1-dependent pathway. *Arterioscler Thromb Vasc Biol.* 2009; 29:254–260. [PubMed: 19023092]
5. Harley SL, Sturge J, Powell JT. Regulation by fibrinogen and its products of intercellular adhesion molecule-1 expression in human saphenous vein endothelial cells. *Arterioscler Thromb Vasc Biol.* 2000; 20:652–658. [PubMed: 10712387]



6. Muro S, Wiewrodt R, Thomas A, Koniaris L, Albelda SM, Muzykantov VR, Koval M. A novel endocytic pathway induced by clustering endothelial ICAM-1 or PECAM-1. *J Cell Sci.* 2003; 116:1599–1609. [PubMed: 12640043]
7. Hsu J, Serrano D, Bhowmick T, Kumar K, Shen Y, Kuo YC, Garnacho C, Muro S. Enhanced endothelial delivery and biochemical effects of alpha-galactosidase by ICAM-1-targeted nanocarriers for Fabry disease. *Journal of Controlled Release.* 2011; 149:323–331. [PubMed: 21047542]
8. Garnacho C, Dhimi R, Simone E, Dziubla T, Lefterovich J, Schuchman EH, Muzykantov V, Muro S. Delivery of acid sphingomyelinase in normal and niemann-pick disease mice using intercellular adhesion molecule-1-targeted polymer nanocarriers. *J Pharmacol Exp Ther.* 2008; 325:400–408. [PubMed: 18287213]
9. Muro S, Garnacho C, Champion JA, Lefterovich J, Gajewski C, Schuchman EH, Mitragotri S, Muzykantov VR. Control of endothelial targeting and intracellular delivery of therapeutic enzymes by modulating the size and shape of ICAM-1-targeted carriers. *Mol Ther.* 2008; 16:1450–1458. [PubMed: 18560419]
10. Muro S, Schuchman EH, Muzykantov VR. Lysosomal enzyme delivery by ICAM-1-targeted nanocarriers bypassing glycosylation- and clathrin-dependent endocytosis. *Mol Ther.* 2006; 13:135–141. [PubMed: 16153895]
11. Muro S, Gajewski C, Koval M, Muzykantov VR. ICAM-1 recycling in endothelial cells: a novel pathway for sustained intracellular delivery and prolonged effects of drugs. *Blood.* 2005; 105:650–658. [PubMed: 15367437]
12. Stan RV. Endocytosis pathways in endothelium: how many? *Am J Physiol Lung Cell Mol Physiol.* 2006; 290:L806–L808. [PubMed: 16603594]
13. Mayor S, Pagano RE. Pathways of clathrin-independent endocytosis. *Nat Rev Mol Cell Biol.* 2007; 8:603–612. [PubMed: 17609668]
14. Grimmer S, van Deurs B, Sandvig K. Membrane ruffling and macropinocytosis in A431 cells require cholesterol. *J Cell Sci.* 2002; 115:2953–2962. [PubMed: 12082155]
15. Lee E, Knecht DA. Visualization of actin dynamics during macropinocytosis and exocytosis. *Traffic.* 2002; 3:186–192. [PubMed: 11886589]
16. Kessner S, Krause A, Rothe U, Bendas G. Investigation of the cellular uptake of E-Selectin-targeted immunoliposomes by activated human endothelial cells. *Biochim Biophys Acta.* 2001; 1514:177–190. [PubMed: 11557019]
17. Straley KS, Green SA. Rapid transport of internalized P-selectin to late endosomes and the TGN: roles in regulating cell surface expression and recycling to secretory granules. *J Cell Biol.* 2000; 151:107–116. [PubMed: 11018057]
18. Ricard I, Payet MD, Dupuis G. VCAM-1 is internalized by a clathrin-related pathway in human endothelial cells but its alpha 4 beta 1 integrin counter-receptor remains associated with the plasma membrane in human T lymphocytes. *Eur J Immunol.* 1998; 28:1708–1718. [PubMed: 9603478]
19. Teasdale MS, Bird CH, Bird P. Internalization of the anticoagulant thrombomodulin is constitutive and does not require a signal in the cytoplasmic domain. *Immunol Cell Biol.* 1994; 72:480–488. [PubMed: 7698819]
20. Murakami M, Horowitz A, Tang S, Ware JA, Simons M. Protein kinase C (PKC) delta regulates PKCalpha activity in a Syndecan-4-dependent manner. *J Biol Chem.* 2002; 277:20367–20371. [PubMed: 11916978]
21. Muro S, Mateescu M, Gajewski C, Robinson M, Muzykantov VR, Koval M. Control of intracellular trafficking of ICAM-1-targeted nanocarriers by endothelial Na<sup>+</sup>/H<sup>+</sup> exchanger proteins. *Am J Physiol Lung Cell Mol Physiol.* 2006; 290:L809–L817. [PubMed: 16299052]
22. Denker SP, Huang DC, Orłowski J, Furthmayr H, Barber DL. Direct binding of the Na<sup>+</sup>-H exchanger NHE1 to ERM proteins regulates the cortical cytoskeleton and cell shape independently of H<sup>(+)</sup> translocation. *Mol Cell.* 2000; 6:1425–1436. [PubMed: 11163215]
23. Oh H-M, Lee S, Na B-R, Wee H, Kim S-H, Choi S-C, Lee K-M, Jun C-D. RKIKK motif in the intracellular domain is critical for spatial and dynamic organization of ICAM-1: functional implication for the leukocyte adhesion and transmigration. *Mol Biol Cell.* 2007; 18:2322–2335. [PubMed: 17429072]

24. Barreiro O, Yanez-Mo M, Serrador JM, Montoya MC, Vicente-Manzanares M, Tejedor R, Furthmayr H, Sanchez-Madrid F. Dynamic interaction of VCAM-1 and ICAM-1 with moesin and ezrin in a novel endothelial docking structure for adherent leukocytes. *The Journal of Cell Biology*. 2002; 157:1233–1245. [PubMed: 12082081]
25. Horinouchi K, Erlich S, Perl DP, Ferlinz K, Bisgaier CL, Sandhoff K, Desnick RJ, Stewart CL, Schuchman EH. Acid sphingomyelinase deficient mice: a model of types A and B Niemann-Pick disease. *Nat Genet*. 1995; 10:288–293. [PubMed: 7670466]
26. Dong QG, Bernasconi S, Lostaglio S, De Calmanovici RW, Martin-Padura I, Breviario F, Garlanda C, Ramponi S, Mantovani A, Vecchi A. A general strategy for isolation of endothelial cells from murine tissues. Characterization of two endothelial cell lines from the murine lung and subcutaneous sponge implants. *Arteriosclerosis, Thrombosis, and Vascular Biology*. 1997; 17:1599–1604.
27. Calderon AJ, Bhowmick T, Leferovich J, Burman B, Pichette B, Muzykantov V, Eckmann DM, Muro S. Optimizing endothelial targeting by modulating the antibody density and particle concentration of anti-ICAM coated carriers. *J Control Release*. 2011; 150:37–44. [PubMed: 21047540]
28. Muro S, Dziubla T, Qiu W, Leferovich J, Cui X, Berk E, Muzykantov VR. Endothelial targeting of high-affinity multivalent polymer nanocarriers directed to intercellular adhesion molecule 1. *J Pharmacol Exp Ther*. 2006; 317:1161–1169. [PubMed: 16505161]
29. Bhowmick T, Berk E, Cui X, Muzykantov VR, Muro S. Effect of flow on endothelial endocytosis of nanocarriers targeted to ICAM-1. *J Control Release*. 2011 In press.
30. Amos C, Romero IA, Schultze C, Rousell J, Pearson JD, Greenwood J, Adamson P. Cross-linking of brain endothelial intercellular adhesion molecule (ICAM)-1 induces association of ICAM-1 with detergent-insoluble cytoskeletal fraction. *Arterioscler Thromb Vasc Biol*. 2001; 21:810–816. [PubMed: 11348879]
31. Tabas I. Secretory sphingomyelinase. *Chem Phys Lipids*. 1999; 102:123–130. [PubMed: 11001566]
32. Bollinger CR, Teichgräber V, Gulbins E. Ceramide-enriched membrane domains. *Biochim Biophys Acta*. 2005; 1746:284–294. [PubMed: 16226325]
33. Holopainen JM, Subramanian M, Kinnunen PK. Sphingomyelinase induces lipid microdomain formation in a fluid phosphatidylcholine/sphingomyelin membrane. *Biochemistry*. 1998; 37:17562–17570. [PubMed: 9860872]
34. Holopainen JM, Angelova MI, Kinnunen PK. Vectorial budding of vesicles by asymmetrical enzymatic formation of ceramide in giant liposomes. *Biophys J*. 2000; 78:830–838. [PubMed: 10653795]
35. Zha X, Pierini LM, Leopold PL, Skiba PJ, Tabas I, Maxfield FR. Sphingomyelinase treatment induces ATP-independent endocytosis. *The Journal of Cell Biology*. 1998; 140:39–47. [PubMed: 9425152]
36. Tam C, Idone V, Devlin C, Fernandes MC, Flannery A, He X, Schuchman E, Tabas I, Andrews NW. Exocytosis of acid sphingomyelinase by wounded cells promotes endocytosis and plasma membrane repair. *The Journal of Cell Biology*. 2010; 189:1027–1038. [PubMed: 20530211]
37. Hanna AN, Berthiaume LG, Kikuchi Y, Begg D, Bourgoin S, Brindley DN. Tumor necrosis factor- $\alpha$  induces stress fiber formation through ceramide production: role of sphingosine kinase. *Mol Biol Cell*. 2001; 12:3618–3630. [PubMed: 11694593]
38. Zeidan YH, Jenkins RW, Hannun YA. Remodeling of cellular cytoskeleton by the acid sphingomyelinase/ceramide pathway. *The Journal of Cell Biology*. 2008; 181:335–350. [PubMed: 18426979]
39. Schuchman EH. Acid sphingomyelinase, cell membranes and human disease: lessons from Niemann-Pick disease. *FEBS Lett*. 2010; 584:1895–1900. [PubMed: 19944693]
40. Liu G, Vogel SM, Gao X, Javaid K, Hu G, Danilov SM, Malik AB, Minshall RD. Src phosphorylation of endothelial cell surface intercellular adhesion molecule-1 mediates neutrophil adhesion and contributes to the mechanism of lung inflammation. *Arterioscler Thromb Vasc Biol*. 2011; 31:1342–1350. [PubMed: 21474822]

41. Yang L, Kowalski JR, Yacono P, Bajmoczy M, Shaw SK, Froio RM, Golan DE, Thomas SM, Lusinskas FW. Endothelial cell cortactin coordinates intercellular adhesion molecule-1 clustering and actin cytoskeleton remodeling during polymorphonuclear leukocyte adhesion and transmigration. *J Immunol.* 2006; 177:6440–6449. [PubMed: 17056576]
42. Ley K, Laudanna C, Cybulsky MI, Nourshargh S. Getting to the site of inflammation: the leukocyte adhesion cascade updated. *Nat Rev Immunol.* 2007; 7:678–689. [PubMed: 17717539]
43. Andrews NW. Regulated secretion of conventional lysosomes. *Trends Cell Biol.* 2000; 10:316–321. [PubMed: 10884683]
44. Canals D, Jenkins RW, Roddy P, Hernandez-Corbacho MJ, Obeid LM, Hannun YA. Differential effects of ceramide and sphingosine 1-phosphate on ERM phosphorylation: probing sphingolipid signaling at the outer plasma membrane. *J Biol Chem.* 2010; 285:32476–32485. [PubMed: 20679347]
45. Hillebrand U, Hausberg M, Stock C, Shahin V, Nikova D, Riethmüller C, Kliche K, Ludwig T, Schillers H, Schneider SW, Oberleithner H. 17beta-estradiol increases volume, apical surface and elasticity of human endothelium mediated by Na<sup>+</sup>/H<sup>+</sup> exchange. *Cardiovasc Res.* 2006; 69:916–924. [PubMed: 16412402]
46. Bourguignon LYW, Singleton PA, Diedrich F, Stern R, Gilad E. CD44 interaction with Na<sup>+</sup>-H<sup>+</sup> exchanger (NHE1) creates acidic microenvironments leading to hyaluronidase-2 and cathepsin B activation and breast tumor cell invasion. *J Biol Chem.* 2004; 279:26991–27007. [PubMed: 15090545]
47. Rebillard A, Tekpli X, Meurette O, Sergent O, LeMoigne-Muller G, Vernhet L, Gorria M, Chevanne M, Christmann M, Kaina B, Counillon L, Gulbins E, Lagadic-Gossmann D, Dimanche-Boitrel M-T. Cisplatin-induced apoptosis involves membrane fluidification via inhibition of NHE1 in human colon cancer cells. *Cancer Res.* 2007; 67:7865–7874. [PubMed: 17699793]
48. Murciano JC, Muro S, Koniaris L, Christofidou-Solomidou M, Harshaw DW, Albelda SM, Granger DN, Cines DB, Muzykantov VR. ICAM-directed vascular immunotargeting of antithrombotic agents to the endothelial luminal surface. *Blood.* 2003; 101:3977–3984. [PubMed: 12531816]
49. Jenkins RW, Canals D, Hannun YA. Roles and regulation of secretory and lysosomal acid sphingomyelinase. *Cell Signal.* 2009; 21:836–846. [PubMed: 19385042]
50. Devlin CM, Leventhal AR, Kuriakose G, Schuchman EH, Williams KJ, Tabas I. Acid sphingomyelinase promotes lipoprotein retention within early atheromata and accelerates lesion progression. *Arterioscler Thromb Vasc Biol.* 2008; 28:1723–1730. [PubMed: 18669882]
51. Marathe S, Schissel SL, Yellin MJ, Beatini N, Mintzer R, Williams KJ, Tabas I. Human vascular endothelial cells are a rich and regulatable source of secretory sphingomyelinase. Implications for early atherogenesis and ceramide-mediated cell signaling. *J Biol Chem.* 1998; 273:4081–4088. [PubMed: 9461601]
52. Altura BM, Gebrewold A, Zheng T, Altura BT. Sphingomyelinase and ceramide analogs induce vasoconstriction and leukocyte-endothelial interactions in cerebral venules in the intact rat brain: Insight into mechanisms and possible relation to brain injury and stroke. *Brain Res Bull.* 2002; 58:271–278. [PubMed: 12128152]
53. Jin S, Zhang Y, Yi F, Li PL. Critical role of lipid raft redox signaling platforms in endostatin-induced coronary endothelial dysfunction. *Arterioscler Thromb Vasc Biol.* 2008; 28:485–490. [PubMed: 18162606]
54. Dhami R, He X, Schuchman EH. Acid sphingomyelinase deficiency attenuates bleomycin-induced lung inflammation and fibrosis in mice. *Cell Physiol Biochem.* 2010; 26:749–760. [PubMed: 21063112]
55. Teichgräber V, Ulrich M, Endlich N, Riethmüller J, Wilker B, De Oliveira-Munding CC, van Heeckeren AM, Barr ML, von Kürthy G, Schmid KW, Weller M, Tümmler B, Lang F, Grassme H, Döring G, Gulbins E. Ceramide accumulation mediates inflammation, cell death and infection susceptibility in cystic fibrosis. *Nat Med.* 2008; 14:382–391. [PubMed: 18376404]

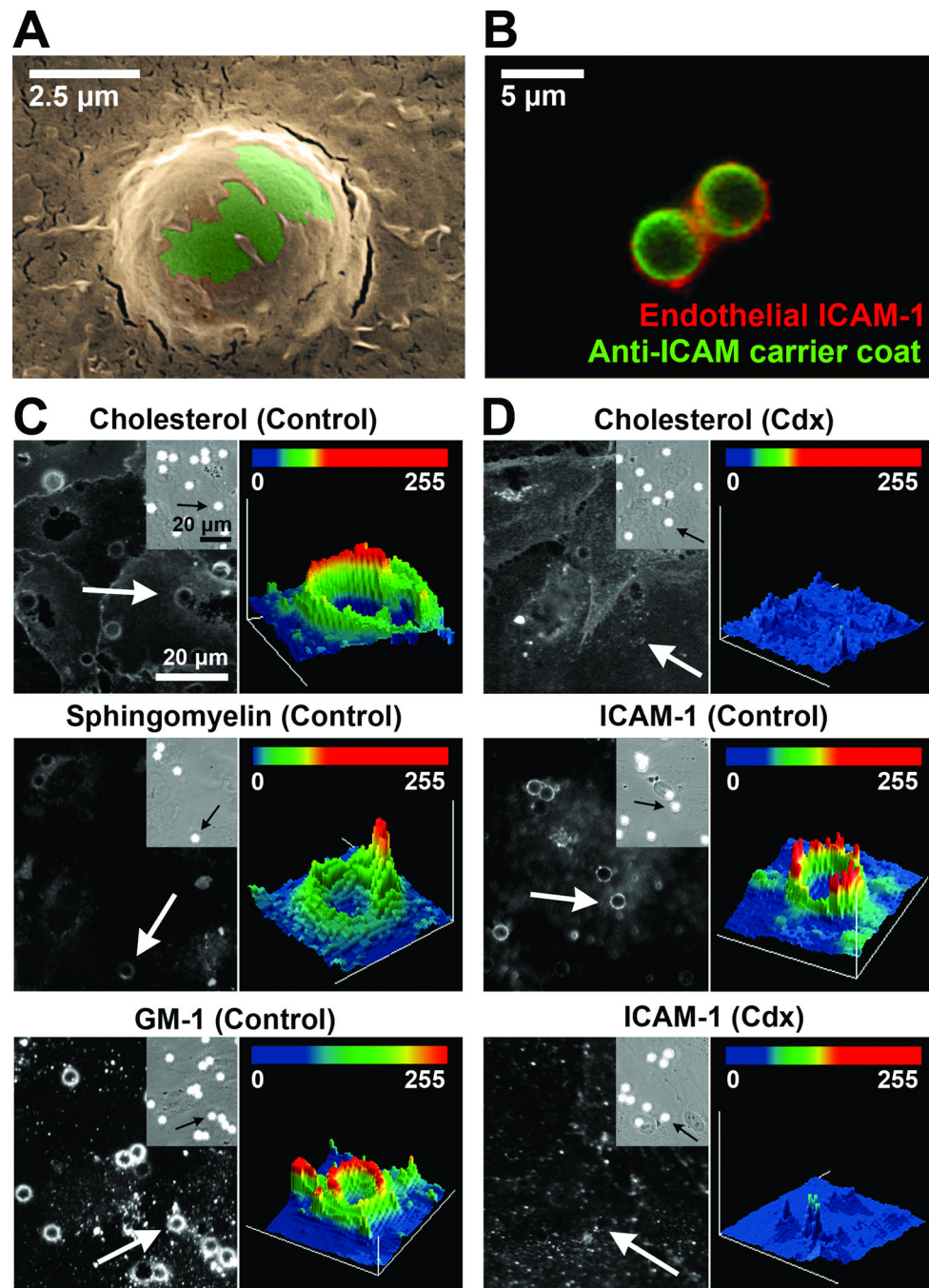


**Figure 1. Enrichment of molecules at sites of anti-ICAM carrier engulfment by ECs**  
 (A) SEM image of a carrier (green) being engulfed by an EC (ochre). Scale bar = 2.5  $\mu\text{m}$ .  
 Fluorescence micrograph showing a carrier (green) being engulfed by ICAM-1-enriched  
 areas of the plasmalemma (red). Scale bar = 5  $\mu\text{m}$ . (C) Fluorescence microscopy images  
 (left panels) and intensity plots (right panels) of carriers marked by arrows, showing  
 enrichment of cholesterol, sphingomyelin, and ganglioside GM1 at carrier-binding sites. (D)  
 Effect of methyl- $\beta$ -cyclodextrin (Cdx) on the enrichment of cholesterol or ICAM-1 at  
 carrier-binding regions. Insets in (C) and (D) show bound carriers by phase-contrast. Scale  
 bars = 20  $\mu\text{m}$ .



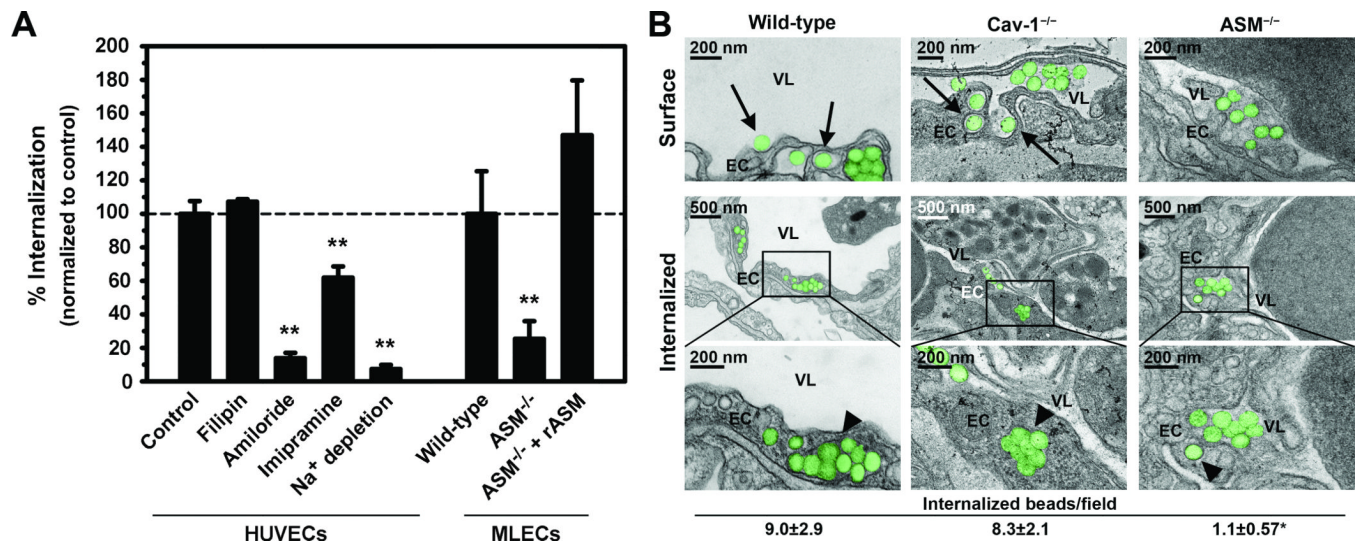


**Figure 2. CAM-mediated endocytosis in cell culture and *in vivo***

(A) Internalization of anti-ICAM carriers (or carriers coated with anti-ICAM and recombinant ASM; rASM) by HUVECs incubated in the absence or presence of pharmacological inhibitors, or MLECs isolated from wild-type or ASM<sup>-/-</sup> mice, was assessed by fluorescence microscopy using a method to counter-stain surface-located carriers, whereas all cell-associated carriers were visualized by phase-contrast. (B) TEM of lung capillaries showing carriers (colorized in green) being engulfed by ECs (arrows) and fully internalized within intracellular vesicles (arrowheads), after intravenous injection of ~180-nm anti-ICAM carriers in wild-type, caveolin-1<sup>-/-</sup>, or ASM<sup>-/-</sup> mice. EC = endothelial cell, VL = vessel lumen. Scale bars = 200 nm or 500 nm, as indicated. The number of carriers/field internalized within ECs was also quantified. Data are mean and s.e.m. (n ≥ 10 micrographs). \*,  $P \leq 0.05$  and \*\*,  $P \leq 0.001$  by Student's *t* test.



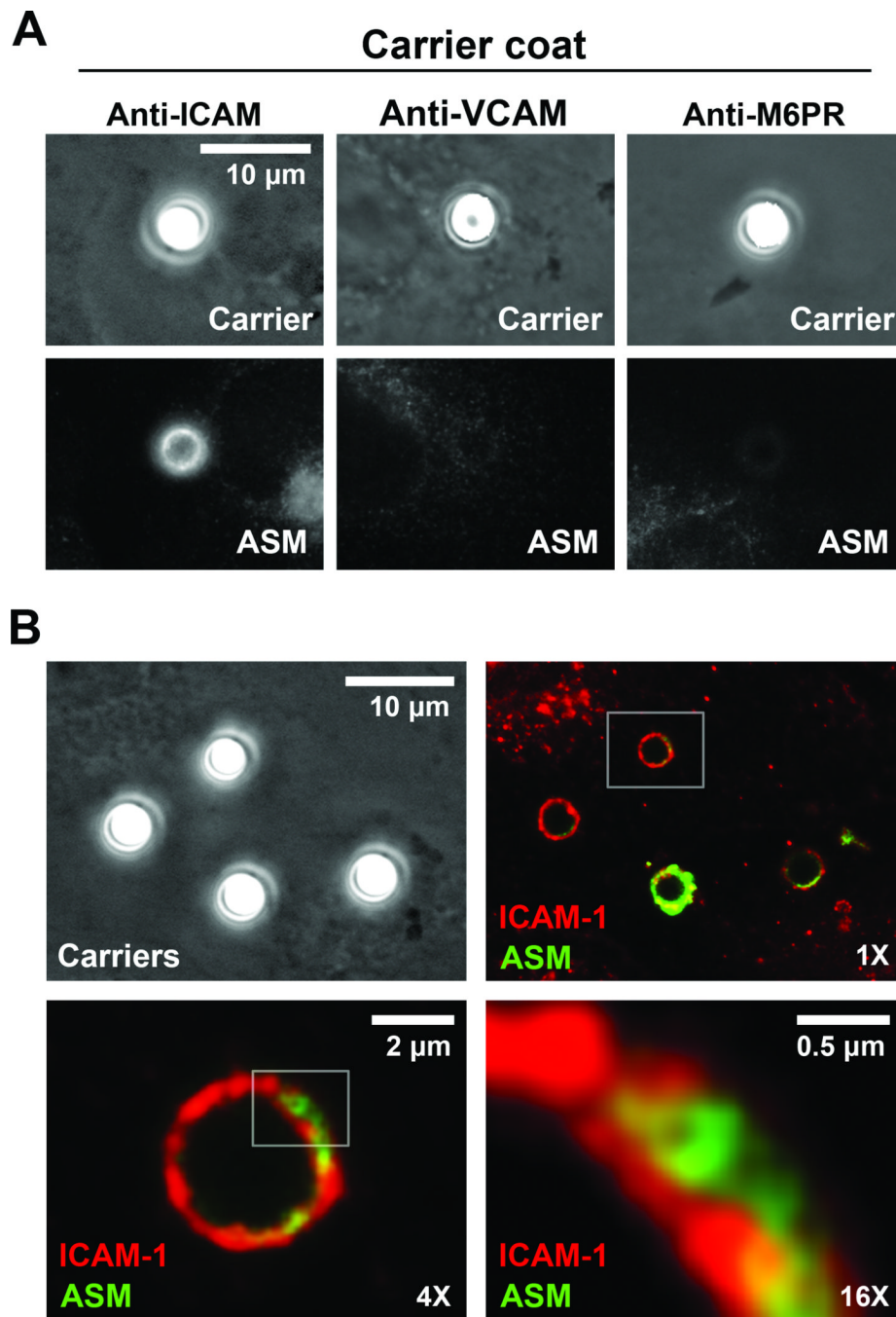


**Figure 3. Distribution of ASM upon engagement of ICAM-1 by anti-ICAM carriers**  
 (A) Fluorescence immunostaining showing ASM (bottom panels) in regions where anti-ICAM, anti-VCAM or anti-M6PR carriers bind to HUVECs (phase-contrast, top panels). Scale bar = 10  $\mu$ m. (B) Fluorescence microscopy showing immunostaining of ASM (green) and ICAM-1 (red) in cells incubated with anti-ICAM carriers. Boxes indicate regions selected for enlargement. Scale bars = 10  $\mu$ m in phase-contrast panel, 2  $\mu$ m in 4X panel, and 0.5  $\mu$ m in 16 X panel.

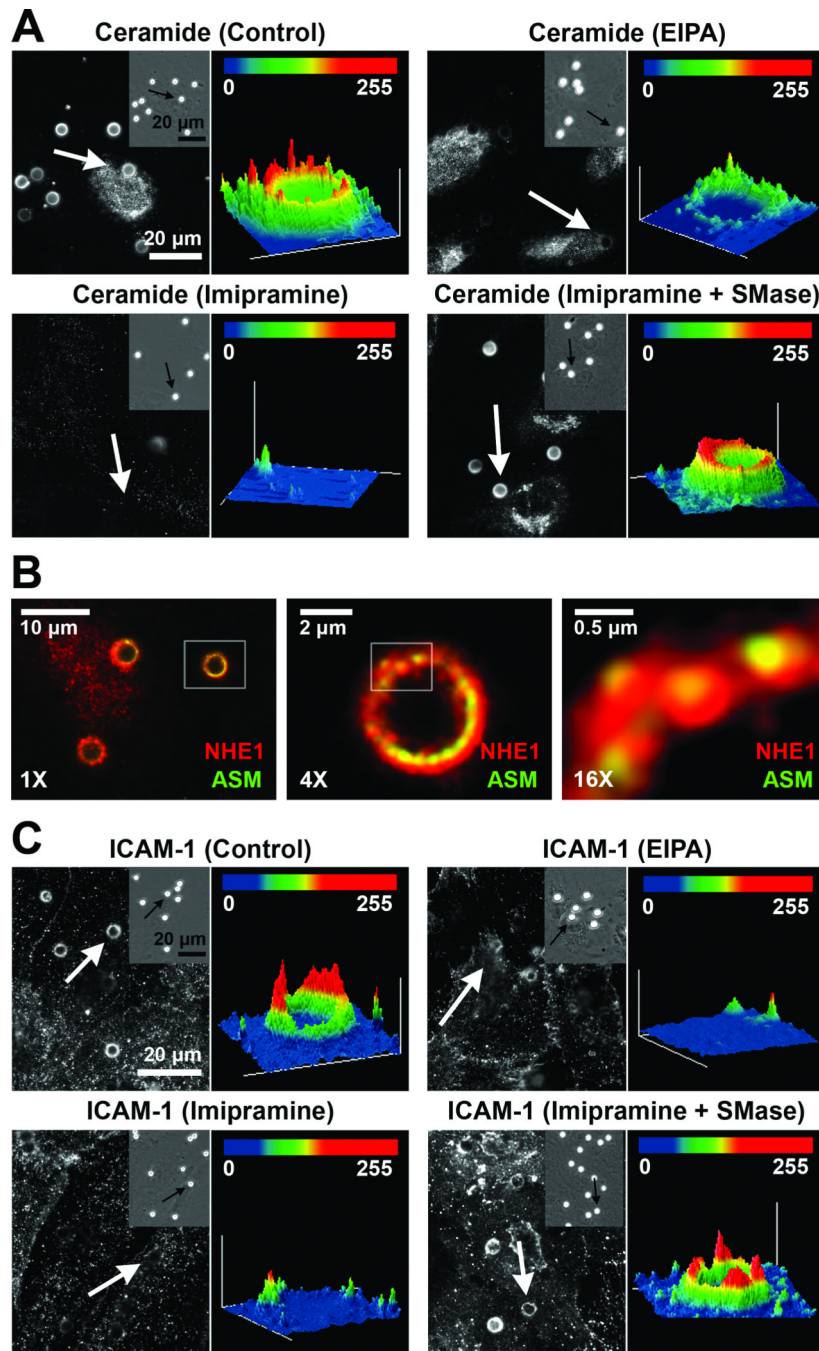


**Figure 4. Ceramide enrichment, and contribution of ASM and NHE1 to engulfment of anti-ICAM carriers by ECs**

(A, C) Fluorescence microscopy images (left sub-panels) and intensity plots (right sub-panels) of the enrichment of ceramide (A) or ICAM-1 (C) in regions of binding of anti-ICAM carriers, marked by arrows, to control, EIPA-treated, imipramine-treated, or imipramine+neutral SM-treated HUVECs. Insets show cell-bound carriers by phase-contrast. Scale bars = 20  $\mu$ m (B) Fluorescence microscopy showing immunostaining of ASM (green) and NHE1 (red) co-localizing at carrier-binding sites. Boxes indicate regions selected for enlargement. Scale bars = 10  $\mu$ m in 1X panel, 2  $\mu$ m in 4X panel, and 0.5  $\mu$ m in 16 X panel.

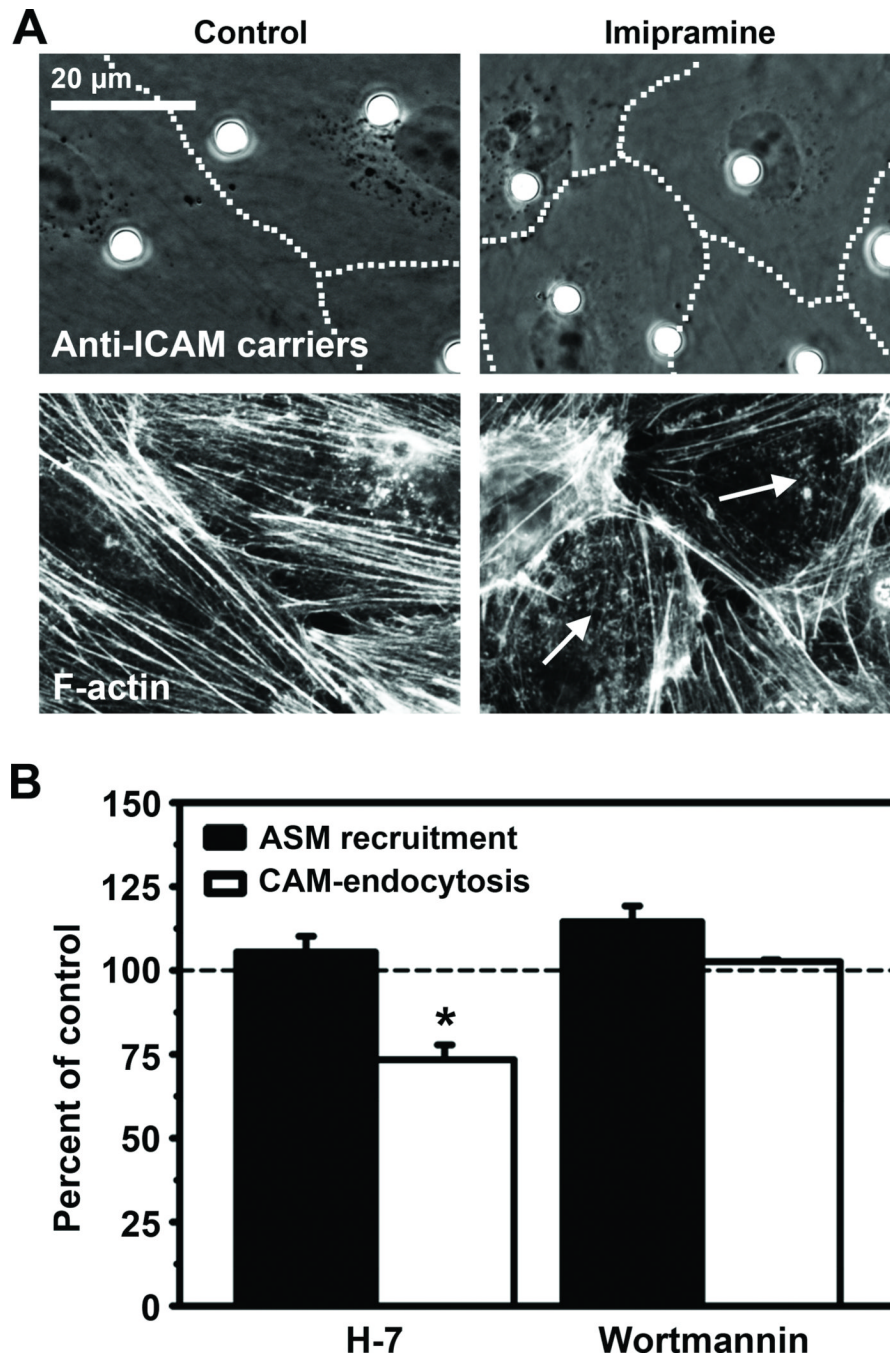


**Figure 5. Recruitment of ASM and actin cytoskeleton-associated signaling upon ICAM-1 engagement**

(A) Phase-contrast micrographs (top panels; dashed lines mark cell borders) of anti-ICAM carriers bound to control or imipramine-treated HUVECs, and the corresponding fluorescence micrographs of F-actin (bottom panels; arrows show disruption of actin stress fibers). Scale bar = 20  $\mu$ m. (B) ASM-positive engulfment structures (black bars) and endocytosis (white bars) of anti-ICAM carriers by control, H-7-treated, or wortmannin-treated HUVECs. Data are normalized to control and represent mean and s.e.m. ( $n \geq 20$  cells). \*,  $P \leq 0.01$  by Student's  $t$  test.

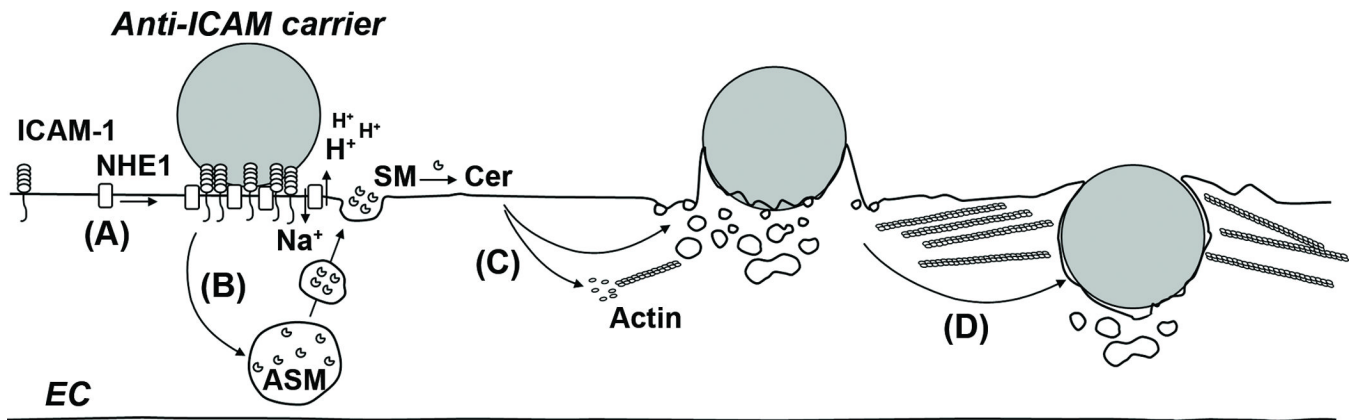


**Figure 6. Model for the association between CAM-mediated endocytosis and the sphingomyelin/ceramide pathway**

(A) Binding of anti-ICAM carriers to ICAM-1 at cholesterol and SM-rich areas of the EC plasmalemma results in recruitment of NHE1, which then interacts with ICAM-1<sup>21</sup>. (B) Binding of carriers to ICAM-1 also induces redistribution of ASM from intracellular compartments to the EC surface. H<sup>+</sup> extrusion by NHE1 at sites of ICAM-1 engagement creates a pH microenvironment optimal for ASM activity, where SM is hydrolyzed to ceramide (Cer). (C) Ceramide induces rearrangement of the actin cytoskeleton, and favors the formation of endothelial engulfment structures and endocytic vesicles at these sites. (D) Uptake of anti-ICAM carriers by cell adhesion molecule- (CAM)-mediated endocytosis occurs.